Effective wall thickness of a single-walled carbon nanotube

T. Vodenitcharova and L. C. Zhang*
School of Aerospace, Mechanical and Mechatronic Engineering, The University of Sydney, NSW 2006, Australia
(Received 9 May 2003; published 2 October 2003)

This paper investigates the effective wall thickness of a single-walled carbon nanotube, a critical quantity for any research in mechanics and property characterization of carbon nanotubes. To this end, the response of a bundle of single-walled carbon nanotubes to external hydrostatic pressure was modeled using the ring theory of continuum mechanics. The model predicted that the equivalent thickness should be 0.617 Å. This in turn clarified the dilemma of the inconsistent Young's modulus of carbon nanotubes reported in the literature.

DOI: 10.1103/PhysRevB.68.165401 PACS number(s): 61.46.+w, 62.25.+g, 46.70.−p

I. INTRODUCTION

Since the discovery of carbon nanotubes a large number of experiments[1–3] and molecular dynamic (MD) simulations[4–6] were conducted on single-walled nanotubes (SWNT's) and multiwalled nanotubes (MWNT's). Notwithstanding their small size, discrete molecular structure, and wall thickness comprised of only a single layer of atoms, carbon nanotubes were found to behave similar to continuum structures and possess both membrane and bending capacities. Thus, it became eminent that equivalent continuum models, as a well established, faster and cheaper option, could be most useful in the analysis and prediction of the behavior of nanotubes. This led to extensive studies on the equivalent or effective properties and geometrical dimensions of a carbon nanotube, i.e., wall thickness h, Young's modulus E, and Poisson's ratio μ. Nevertheless, the mechanics modeling so far has been associated with strong assumptions. For example, a carbon nanotube has been treated as a truss member,[7] a beam,[8] a thin shell,[6,9–12] or a solid cylinder.[8,13,14]

To date, there is no agreement about the exact values of h, E, and μ of a carbon nanotube. Some studies assumed that a nanotube was a solid cylinder.[8,13,14] Others considered that h was equal to the interplanar spacing of graphite layers $d_g = 3.4$ Å.[2–4,11,15–19] The equivalent Young's modulus was then calculated based on this h value. While such an assumption, $h = d_g$, has its merit for MWNT's, it is rather ambiguous for SWNT's. In contrast, Yakobson and co-workers[6] derived a much smaller value of $h = 0.66$ Å in the case of SWNT's through the calculation of the flexural rigidity $Eh^3/12(1-\mu^2)$ and in-plane stiffness Eh using the Tersoff-Brenner potential, which is only one fifth of the commonly adopted $h = 3.4$ Å. The Young's modulus of a carbon nanotube was also reported to have a variety of values, ranging from 0.27 TPa for MWNT's (Ref. 3) to 5.5 TPa for SWNT's,[6] although most agreed that E was about 1 to 2 TPa.[1,8,17] The discrepancy in the values of the Poisson's ratio μ reported in the literature was also big, varying from as low as 0.12 (Ref. 20) to as large as 0.28.[18] It needs to be emphasized that the inconsistency in the determination of the values of E is intrinsically related to the assumption of the equivalent wall thickness.

Predominantly, the continuum mechanics theories for carbon nanotubes were applied to bending,[8,13] axial tension,[2,3] and axial compression;[9–12,14,21] a few studies have been done on radial compression.[19,22–26] Tang and co-workers[26] tested SWNT bundles in a diamond anvil cell under a hydrostatic pressure up to 1.5 GPa [Fig. 1(a)] and measured the radial deformation in terms of the lattice constant ξ, i.e., the center-to-center distance between the nanotubes. They found that ξ linearly decreased with the external pressure. They also carried out theoretical calculations based on the Lennard- Jones potential. The values of ξ were reported to be in good agreement with the experiments. The present study will develop a continuum mechanics model to predict the effective thickness of a single-walled carbon nanotube and to discuss its Young's modulus.

II. MODELING AND PREDICTION

Consider the deformation of the central nanotube in a bundle of SWNT's subjected to an external pressure q [Fig. 1(a)]. It is postulated that the external pressure is transmitted to the central nanotube through the surrounding ones. As the external pressure compresses the bundle, the exterior tubes deform and the intertubular distance d decreases, inducing repulsive intertubular van der Waals forces. Since the distance between the atoms of two neighboring tubes varies circumferentially, the van der Waals forces must also vary. It is hence reasonable to assume that the van der Waals forces have a maximum value at the location with the shortest distance d [Fig. 1(b)].

Further, the compressive pressure between the tubes is considered to be $p_{\text{atm}}+p_0 \sin^2(3\theta)$, which produces the faceting observed in experiments,[26] and hence is consistent with the experimental loading conditions. The magnitude p_0 is determined by equating the total load applied on one sixth of the circumference of an exterior tube and the total load applied on 1/6th of the circumference of the central tube [Fig. 1(b)], i.e.,

$$\frac{q(2\pi R)}{6} = \int_0^{2\pi R/6} p_0 \sin^2(3\theta)\, ds, \tag{1}$$

which leads to

$$p_0 = 2q. \tag{2}$$

As a result, the total radial load on one tube is the same as if the tube were submerged into the pressure medium in an isolated state.

Since the nanotubes in a bundle are long and the load along the tube axis is quite uniform, a nanotube is under plane-strain deformation and can be modeled as a thin ring with a mean radius R, a thickness h in the radial direction, and a unit width in the axial direction [Fig. 1(c)]. When the external pressure is statically applied and the material is linearly elastic, the radial and tangential displacements of the ring under small deformation, w and v, can be described as (see the Appendix for derivation details):

$$w(\theta) = W_0 + W_n \cos(n\theta),$$

$$v(\theta) = V_n \sin(n\theta), \tag{3}$$

where $n=6$ and W_n and $V_n$are defined in Eq. (A6). The above equation shows that the radial deformation is described by six circumferential waves. The wavy pattern of the radial displacement distorts the initial circular cross section of the tube.

Tang *et al.*[26] reported two measures for the faceting of a nanotube cross section: (1) a distortion ratio η, which is the ratio of the shortest radius $r^{(<)}$ to the longest radius $r^{(>)}$ [see their definitions in Fig. 1(b) and Eq. (A7)] and (2) the lattice constant ξ, which is the center-to-center distance between the tubes [defined in Fig. 1(a) and Eq. (A8)]. At the zero external pressure it was found that $\eta_0 = 0.991$ and $\xi_0 = 17.13$ Å. At the maximum external pressure $q = 1.5$ GPa in their test, $\eta_{1.5\ \mathrm{GPa}} = 0.982$ and $\xi_{1.5\ \mathrm{GPa}} = 16.89$ Å. These measured parameters can be used to determine the unknown parameters h, E, and R in the model derived above.

Applying Eqs. (A9) and (A10), the longest and shortest radii at zero external pressure are obtained as $r_0^{(>)} = 7.073$ Å and $r_0^{(<)} = 7.0096$ Å. When the external pressure becomes 1.5 GPa, $r_{1.5}^{(>)} = 7.08$ Å and $r_{1.5}^{(<)} = 6.953$ Å. Equation (A11) then gives rise to $W_{n,0} = 0.03183$ Å, $R + W_{0,0} = 7.041$ Å, $W_{n,1.5} = 0.06372$ Å, and $R + W_{0,1.5} = 7.0167$ Å. On the other hand, Eq. (A13) leads to $R/h = 11.446$ and hence $R = 7.066$ Å according to Eq. (A15). Thus, the ring thickness is predicted to be $h = 0.617$ Å, which is 43.8% of the theoretical diameter of a carbon atom (1.42 Å) and is close to the thickness 0.66 Å calculated by Yakobson *et al.*[6] by MD simulations. With the known R/h, Eq. (A14) yields $R/E = 1.44675\ (10^{-13}\ \mathrm{mm}^3/\mathrm{N})$. Thus, the Young's modulus of the nanotube is 4.88 TPa, which is also close to the molecular dynamics estimation of 5.5 TPa.[6] Having the geometrical and material parameters, one can obtain the generalized degrees of freedom W_n and V_n varying with the external pressure. The lattice constant ξ can therefore be determined by Eq. (A8). Figure 2 shows that the model prediction is identical to the MD results,[26] which are very close to the experimental measurements.[26] In the calculations, the equilibrium distance between the adjacent nanotubes [Fig. 1(a)] d is the same as given by Tang *et al.*[26]

It is expected that the effective wall thickness of a continuous nanotube must be smaller than the theoretical diameter of a carbon atom. This is understandable when the equilibrium of a nanotube is considered. A cross section of a real nanotube contains only a limited number of atoms. Under an external load, stresses in the tube are transmitted through these atoms, while in a continuum mechanics model the same stresses are transmitted through the continuous wall area. As a result, the wall thickness must be smaller than the atom diameter; otherwise, the tube equilibrium cannot be maintained. In this sense, calculations using continuum models that apply wall thickness greater than or equal to the diameter of a carbon atom, can give incorrect answer.

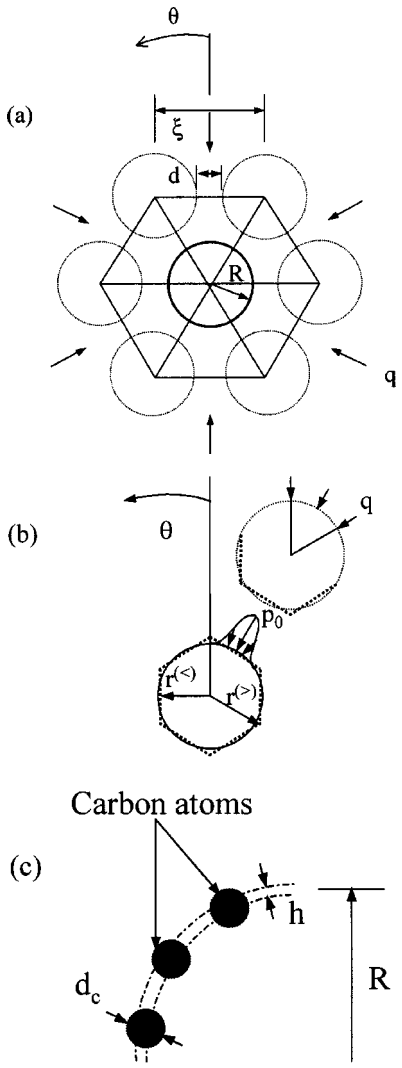

FIG. 1. (a) Nanobundle geometry and external pressure on the entire triangular tube lattice, where R is the radius of an isolated nanotube, ξ the lattice constant, d the equilibrium distance between the nanotubes, θ the circumferential coordinate, and q is the external pressure on the nanobundle. (b) Load on a 1/6th of a nanotube. (c) Partial cross section of a nanotube, where d_c is the theoretical diameter of a carbon atom and h is the equivalent thickness of the nanotube.

The problem of the effective wall thickness outlined above also leads to the problem in the Young's modulus characterization of carbon nanotubes. For instance, when the Young's modulus E is obtained by examining the axial rigidity C of a nanotube, which is proportional to the wall thick-

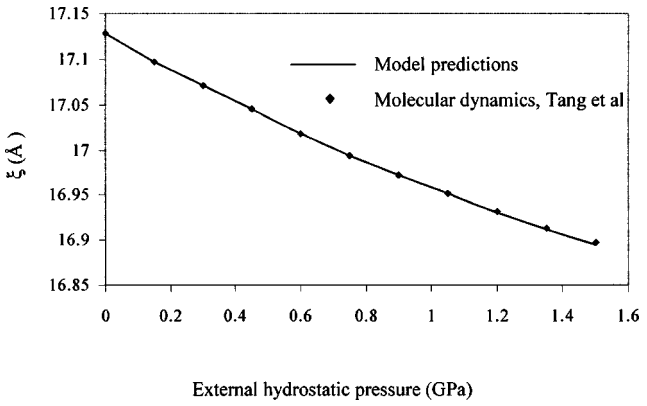

FIG. 2. Lattice constant ξ vs external hydrostatic pressure.

ness ($C \sim Eh$), E cannot be correct if an inappropriate h is used, even when C is accurately measured. If a bending test is used to characterize E, the bending rigidity D, which is proportional to h^3 ($D \sim Eh^3$), is often used. Again, because of the incorrect h, the diverse E values reported in the literature are unavoidable.

SUMMARY

The model developed in the present paper predicts that the effective thickness of a single-walled carbon nanotube is $h = 0.617$ Å, which is 43.8% of the theoretical diameter of a carbon atom, and that the Young's modulus of the tube is 4.88 TPa. The prediction is based on a direct measurement of a nanotube deformation and is reliable. This in turn clarifies the dilemma of the diverse Young's modulus reported previously in the literature.

ACKNOWLEDGEMENT

This work was supported by an ARC Discovery Grant.

APPENDIX

1. Modeling

The radial and tangential displacement components, w and v, of a linear extensional ring can be expressed as

$$w(\theta) = \sum_0^\infty W_n \cos(n\theta),$$

$$v(\theta) = \sum_0^\infty V_n \sin(n\theta), \tag{A1}$$

where an outward w is positive. Considering the displacement boundary conditions of symmetry about $\theta = 0°$ and angles multiple of 30°, the only nonzero radial displacements are those with $n = 0$, 6, 12, 18,..., and the only nonzero tangential displacements are those with $n = 6$, 12, 18,... .

When the ring is under small deformation its circumferential direct strain of the centroidal axis ε and the curvature change of the centroidal axis k are[27]

$$\varepsilon = \frac{v' + w}{R},$$

$$k = \frac{(v - w')'}{R^2}, \tag{A2}$$

where the prime means a derivation with respect to θ. To calculate V_n and W_n in Eq. (A1),the principle of stationary potential energy can be used. This principle states that in static equilibrium the potential energy of the ring $\Pi = U + W$ is minimum, where U is the strain energy and W is the work done by the external load on the ring. The strain energy U in the present case can be determined as

$$U = \frac{1}{2} EAR \int \varepsilon^2 d\theta + \frac{1}{2} EIR \int k^2 d\theta, \tag{A3}$$

where $A = bh$ is the cross-sectional area and $I = bh^3/12$ is the second moment of inertia of the ring cross section. The work done by a pressure normal to the deformed surface (hydrostatic pressure) is only associated with the radial displacement. Hence,

$$W = R \int_0^{2\pi} p(\theta) w d\theta. \tag{A4}$$

The condition for Π being minimum is that its partial derivatives with respect to W_n and V_n are zero, i.e.,

$$\frac{\partial \Pi}{\partial W_0} = 0,$$

$$\frac{\partial \Pi}{\partial W_n} = 0, n = 6,12,18,...,$$

$$\frac{\partial \Pi}{\partial V_n} = 0, n = 6,12,18,... . \tag{A5}$$

This results in a set of simultaneous linear algebraic equations for W_n and V_n, which solved leads to

$$W_0 = -\frac{(p_{\text{atm}} + p_0/2)R^2}{EA},$$

$$W_n = \frac{p_0 R^4}{2EI(n^2-1)^2}\left(1 + \frac{I}{AR^2}\right), \tag{A6}$$

$$V_n = -\frac{p_0 R^2}{2EA(n^2-1)^2}\left(n - \frac{AR^2}{nI}\right),$$

where $n = 6$. Equation (A6) indicates that only the sixth harmonic contributes. The radial displacement distribution represents closely the hexagonal distortion in the cross-sectional area of the individual tubes in the bundle, with flattened sides against each other, as illustrated in Fig. 1(b). Therefore, the variation of the circumferential pressure, governed by $\sin^2(3\theta)$, provides the right displacement distribution observed in both experiments and molecular dynamics simulations. Equation (A6) clearly shows that W_n and V_n depend on R/E and R/h.

2. Parameters determination

The faceting of the cross section is measured[26] in terms of the distortion ratio η and the lattice constant ξ:

$$\eta = \frac{r^{(<)}}{r^{(>)}},$$

$$r^{(<)} = R + W_0 - W_n, \tag{A7}$$

$$r^{(>)} = R + W_0 + W_n$$

$$\xi = 2r^{(<)} + d, \tag{A8}$$

where $r^{(<)}$ is the shortest radius and $r^{(>)}$ is the longest radius of the distorted cross section. If η, ξ, and d are given for a particular load, then from Eqs. (A7), (A8) one can calculate R, W_0, and W_n as explained below. From Eq. (A8) it follows that

$$r^{(<)} = \frac{\xi - d}{2}, \tag{A9}$$

and from Eq. (A7) for a given η

$$r^{(>)} = \frac{r^{(<)}}{\eta}. \tag{A10}$$

With the known $r^{(<)}$ and $r^{(>)}$, Eqs. (A7), (A9), and (A10) lead to

$$W_n = \frac{r^{(>)} - r^{(<)}}{2},$$

$$R + W_0 = \frac{r^{(>)} + r^{(<)}}{2}. \tag{A11}$$

Since the response of the ring is linear, superposition is allowed. The difference between the displacements at zero external pressure, $W_{0,0}$ and $W_{n,0,}$ and those at $p_0 = 1.5$ GPa, $W_{0,1.5}$ and $W_{n,1.5}$, can be expressed as

$$W_{n,q} - W_{n,0} = \frac{p_0}{2b(n^2-1)^2} \frac{R}{E} \frac{R}{h} \left[12 \left(\frac{R}{h} \right)^2 + 1 \right],$$

$$(R + W_{0,q}) - (R + W_{0,0}) = -\frac{p_{\text{atm}} + p_0/2}{b} \frac{R}{E} \frac{R}{h}. \tag{A12}$$

Hence, for $p_{\text{atm}} = 0$ one gets

$$\frac{R}{h} = \left\{ \frac{1}{12} \left[\frac{(n^2-1)^2 (W_{n,q} - W_{n,0})}{(R + W_{0,0}) - (R + W_{0,q})} - 1 \right] \right\}, \tag{A13}$$

$$\frac{R}{E} = 2b \frac{(R + W_{0,0}) - (R + W_{0,q})}{p_0 \dfrac{R}{h}}. \tag{A14}$$

Further, R can be found using Eqs. (A6), (A13)–(A14), i.e.,

$$R = \frac{r_0^{(>)} + r_0^{(<)}}{2} + \frac{r_0^{(>)} - r_0^{(<)}}{2} \frac{(n^2-1)^2}{12 \left(\dfrac{R}{h} \right)^2 + 1}. \tag{A15}$$

With the obtained value of R, the wall thickness h and the Young's modulus E are determined by Eqs. (A13) and (A14), respectively.

*E-mail address: lzha9252@mail.usyd.edu.au

[1] J. P. Salvetat, G. A. D. Briggs, J. M. Bonard, R. R. Bacsa, A. J. Kilik, T. Stockli, N. A. Burnham, and L. Forro, Phys. Rev. Lett. **82**, 944 (1999).

[2] M. F. Yu, B. S. Files, S. Arepalli, and R. S. Ruoff, Phys. Rev. Lett. **84**, 5552 (2000).

[3] M. F. Yu, O. Lourie, M. J. Dyer, K. Moloni, T. F. Kelly, and R. S. Ruoff, Science **287**, 637 (2000).

[4] E. Hernandez, C. Goze, P. Bernier, and A. Rubio, Appl. Phys. A: Mater. Sci. Process. **68**, 287 (1999).

[5] T. Ozaki, Y. Iwasa, and T. Mitani, Phys. Rev. Lett. **84**, 1712 (2000).

[6] B. I. Yakobson, C. J. Brabec, and J. Bernholc, Phys. Rev. Lett. **76**, 2511 (1996).

[7] G. M. Odegard, T. S. Gates, L. M. Nicholson, and K. E. Wise (unpublished).

[8] E. W. Wong, P. E. Sheehan, and C. M. Lieber, Science **277**, 1971 (1997).

[9] C. Q. Ru, Phys. Rev. B **62**, 9973 (2002).

[10] C. Q. Ru, Phys. Rev. B **62**, 10 405 (2000).

[11] C. Q. Ru, J. Appl. Phys. **89**, 3426 (2001).

[12] C. Q. Ru, J. Mech. Phys. Solids **49**, 1265 (2001).

[13] S. Govindjee and J. L. Sackman, Solid State Commun. **110**, 227 (1999).

[14] C. F. Cornwell and L. T. Wille, Solid State Commun. **101**, 555 (1997).

[15] E. Hernandez, C. Goze, P. Bernier, and A. Rubio, Phys. Rev. Lett. **80**, 4502 (1998).

[16] J. P. Lu, Phys. Rev. Lett. **79**, 1297 (1997).

[17] A. Krishnan, E. Dujardin, T. W. Ebbesen, P. N. Yianilos, and M. M. J. Treacy, Phys. Rev. B **58**, 14 013 (1998).

[18] J. P. Lu, J. Phys. Chem. Solids **58**, 1649 (1997).

[19] C. Thomsen, S. Reich, H. Jantoljak, I. Loa, K. Syassen, M. Burghard, G. S. Duesberg, and S. Roth, Appl. Phys. A: Mater. Sci. Process. **69**, 309 (1999).

[20] D. Sanchez-Portal, E. Artacho, and M. J. Soler, Phys. Rev. B **59**, 12 678 (1991).

[21] C. Q. Ru, Phys. Rev. B **62**, 16 962 (2002).

[22] Y. Xia, M. Zhao, Y. Ma, M. Ying, X. Liu, P. Liu, and L. Mei, Phys. Rev. B **65**, 155415 (2002).

[23] S. Reich, C. Thomsen, and P. Ordejon, Phys. Rev. B **65**, 153407 (2002).

[24] S. M. Sharma, S. Karmakar, S. K. Sikka, P. V. Teredesai, A. K. Sood, A. Govindaraj, and C. N. R. Rao, Phys. Rev. B **63**, 205417 (2001).

[25] U. D. Venkateswaran, A. M. Rao, E. Richter, M. Menon, A. Rinzler, R. E. Smalley, and P. C. Eklund, Phys. Rev. B **59**, 10 928 (1999).

[26] J. Tang, L.-C. Qin, T. Sasaki, M. Yudasaka, A. Matsushita, and S. Iijima, Phys. Rev. Lett. **85**, 1887 (2000).

[27] M. Farshad, *Stability of Structures* (Elsevier Science, Amsterdam, 1994).